Journal of Organometallic Chemistry, 426 (1991) 71–86
Elsevier Sequoia S.A., Lausanne
JOM 22306

Synthesis and characterization of various coordination modes of 1,1′-bis(diphenylphosphino)ferrocene in iron carbonyl complexes. X-Ray crystal structures of (η^1-BPPF)Fe(CO)$_4$, (μ,η^2-BPPF)(Fe(CO)$_4$)$_2$, and (μ,η^2-BPPF)Fe$_3$(CO)$_{10}$

Tae-Jeong Kim, Soon-Chul Kwon, Yong-Hoon Kim, Nam Ho Heo
Department of Industrial Chemistry, Kyungpook National University, Taegu 702-701 (South Korea)

Martha M. Teeter and Akihito Yamano
Department of Chemistry, Boston College, Chestnut Hill, MA 02167 (USA)

(Received June 28, 1991)

Abstract

Reactions of 1,1′-bis(diphenylphosphino)ferrocene (BPPF) with Fe$_2$(CO)$_9$ and Fe$_3$(CO)$_{12}$ produced a series of iron carbonyl derivatives: (η^2-BPPF)Fe(CO)$_3$ (**1**), (η^1-BPPF)Fe(CO)$_4$ (**2**), (μ,η^2-BPPF)(Fe(CO)$_4$)$_2$ (**3**), (η^2-BPPF)Fe$_2$(CO)$_7$ (**4**), and (μ,η^2-BPPF)Fe$_3$(CO)$_{10}$ (**5**). The synthesis and characterization of **4** and **5**, including X-ray crystal structures of **2**, **3**, and **5**, confirmed various coordination modes of BPPF. Crystal data are as follows: (η^1-BPPF)Fe(CO)$_4$ (**2**): orthorhombic, space group *Pbca*, $a = 26.27(1)$, $b = 23.18(1)$, $c = 10.938(8)$ Å, $V = 6661(7)$ Å^3, $Z = 8$; 3017 data with $I > 3.0\sigma(I)$ were refined to $R = 0.057$, $R_w = 0.056$; (μ,η^2-BPPF)Fe$_3$(CO)$_{10}$ (**5**): monoclinic, space group $P2_1/n$, $a = 11.231(1)$, $b = 21.043(4)$, $c = 20.373(9)$ Å, $\beta = 97.373(9)°$, $V = 4693(4)$ Å^3, $Z = 4$; 6082 data with $I > 3.0\sigma(I)$ were refined to $R = 0.054$, $R_w = 0.071$; (μ,η^2-BPPF)Fe$_2$(CO)$_8$ (**3**): monoclinic, space group $C2/c$, $a = 17.223(7)$, $b = 14.97(2)$, $c = 18.558(3)$ Å, $\beta = 108.39(3)°$, $V = 4541(6)$ Å^3, $Z = 4$; 3201 data with $I > 3.0\sigma(I)$ were refined to $R = 0.070$, $R_w = 0.139$, as a result of difficulties with modeling electron density peaks associated with highly disordered solvent atoms.

Introduction

Ferrocenylphosphines are now well known as efficient ligands for metal complexes in a wide range of homogeneous catalysis. Upon examination of the literature, it is obvious that much interest has been focused on such reactions as hydrogenation of olefinic substrates [1–6], Grignard cross-coupling reactions [7]

Correspondence to: Dr. T.-J. Kim or Dr. N.H. Heo, Department of Industrial Chemistry, Kyungpook National University, Taegu 702-701, South Korea.

hydrosilylation of ketones [8] and aldol condensation [9,10]. Of various achiral and chiral ferrocenylphosphine ligands, those that have been most widely and effectively used in these catalytic reactions are 1,1'-bis(diphenylphosphino)ferrocene (BPPF), 2-(diphenylphosphino)-1-(*N*,*N*-dimethylaminoethyl)ferrocene (PPFA), and 1',2-bis(diphenylphosphino)-1-(*N*,*N*-dimethylaminoethyl)ferrocene (BPPFA).

Despite wide applications of these ligands in complex formation for use in such catalytic reactions, relatively few studies have been carried out on the preparation and structure of their iron group complexes and their uses in homogeneous catalysis. We have recently reported the catalytic properties of (η^2-BPPF)Fe(CO)$_3$ (**1**), (η^1-BPPF)Fe(CO)$_4$ (**2**), and (μ,η^2-BPPF)(Fe(CO)$_4$)$_2$ (**3**), synthesized as products of the reaction between the ligand BPPF and Fe(CO)$_5$ [11]. They proved to be very efficient catalyst precursors for the synthesis of carbamates from the reaction of propargyl alcohol with secondary amines in the presence of CO_2 [12].

Prompted by these findings, we decided to look further into the reactivity and coordination modes of ligand BPPF with other iron carbonyls such as $Fe_2(CO)_9$ and $Fe_3(CO)_{12}$. It was hoped to see a new series of iron carbonyl derivatives of BPPF with various coordination modes, since from our previous studies we have found that the ligand can act not only as a typical chelating bidentate but as a monodentate diphosphine, or a bridging ligand in dimeric species. Although many instances are now known for the chelating mode of this ligand, the latter two modes of coordination for this ligand have so far been scarce [13,14]. In this work, we report the synthesis of (η^2-BPPF)Fe$_2$(CO)$_7$ (**4**), (μ,η^2-BPPF)Fe$_2$(CO)$_{10}$ (**5**) and crystal structures of iron complexes of BPPF, **2**, **3**, and **5**.

Experimental

Reagents and instruments

All manipulations were conducted under an argon atmosphere using a double manifold vacuum system and Schlenk techniques. All commercial reagents were used as received unless otherwise mentioned. Solvents were purified by standard techniques [15], and were freshly distilled prior to use. Melting points were determined using a Gallenkamp melting point apparatus and are reported without correction. ^{1}H, ^{13}C, and ^{31}P NMR spectra were recorded on a Bruker Am-300 spectrometer operating at 300, 80.15, and 121.5 MHz, respectively. Infrared spectra were recorded on a FT-IR:Bio-RADFTS 20/30 spectrometer. Mass spectra were obtained using a Kratos MS-50 instrument. Microanalyses were performed by Ms. T.Y. Park in the Department of Industrial Chemistry, Kyungpook National University, South Korea.

The ligand BPPF was prepared as described previously [16]. Crystals of diffraction quality of previously reported iron carbonyl complexes **2** and **3** were obtained from hexane/ether mixtures of ratios 5:1 and 3:1, respectively [11].

Preparation of (η^2-BPPF)Fe$_2$(CO)$_7$ (4)

The ligand BPPF (0.98 g, 1.78 mmol) was added to a suspension of $Fe_2(CO)_9$ (0.88 g, 2.41 mmol) in CH_2Cl_2 (30 mL) in a 100 mL Schlenk tube with a magnetic stirrer and an argon inlet. The reaction mixture was stirred for 12 h. The solution was then filtered on a Celite tube to remove any solid impurities, and the brownish orange filtrate was evaporated to dryness. The remaining oily residue was taken up

in a small volume of THF to be chromatographed on silica gel. Three orange bands developed by eluting with mixtures of hexane and ether. After removing the first two bands (**2** and **3**) on elution with hexane/ether (3:1) the third band was eluted with ether to obtain **4** as a yellow powder after removal of solvent. Yield of **4**: 0.02 g, 1.3%. IR (KBr) 2049s, 1971m, 1929vs, 1883s, 1875vs cm^{-1}. Anal. Found: C, 57.67; H, 3.72. (BPPF)$Fe_2(CO)_7$ calc.: C, 57.14: H, 3.28%. Yields of **2** and **3** were 16 and 21%, respectively, based on the ligand.

Preparation of (μ,η^2-*BPPF*)$Fe_3(CO)_{10}$ (**5**)

The title compound was obtained as a minor product along with the compounds **2**, **3**, and **4** from the reaction of BPPF with $Fe_3(CO)_{12}$. $Fe_3(CO)_{12}$ (0.91 g, 1.8 mmol) and BPPF (1.0 g, 1.81 mmol) were dissolved in CH_2Cl_2 (30 mL) in a 100-mL, two-necked, round-bottomed flask with a condenser, a magnetic stirrer, and an argon inlet. The solution was refluxed with stirring for 4 h during which time the solution became dark brown with deposit of black precipitates. The solution was then filtered on a Celite tube to remove the precipitates, and the filtrate evaporated to dryness. The remaining dark brown oily residue was dissolved in a small volume of THF to be chromatographed on silica gel. Four bands developed on elution with mixtures of hexane/ether (5:1) and hexane/ether (3:1), respectively, the third purple band was eluted with a 2:1 mixture of hexane and ether, and **5** obtained as dark purple crystals after removal of solvents followed by crystallization from CH_2Cl_2/ether (1:3) at room temperature. The remaining orange band was eluted with ether to be identified as **4**. Yield of **5**: 0.51 g, 8%. IR (KBr) 2067vs, 1998vs, 1952s, 1782s, 1740s cm^{-1}. Anal. Found: C, 52.92; H, 3.00. (BPPF)$Fe_3(CO)_{10}$ calc.: C, 52.76; H, 2.82%. Yields of **2**, **3**, and **4** were 2, 21, and 6%, respectively.

X-Ray crystallographic analysis of **2**, **3**, *and* **5**

For each compound, a chunky crystal, approximately $0.3 \times 0.3 \times 0.3$ mm, was mounted on a glass fiber. All measurements were made on a Rigaku AFC5R diffractometer with graphite monochromated Mo-K_α radiation ($\lambda = 0.71069$ Å) and 12 kW rotating anode generator. Preliminary experiments for the cell parameters and orientation matrix for each crystal were carried out by least-squares refinement, using the setting angles of 25 carefully centered reflections in the range $20° < 2\theta < 35°$.

For each crystal, diffraction intensities were collected at a constant temperature of 20 ± 1°C using the ω-2θ scan technique with a scan speed of 32°/min (in ω) which is a maximum attainable speed with the diffractometer. Omega scans of several intense reflections were made prior to the data collection to optimize the proper scan width for each crystal. The weak reflections ($I < 10\sigma(I)$) were rescanned (maximum of 3 rescans) and the counts were accumulated to assure good counting statistics. Stationary background counts were recorded on each side of the reflection. The ratio of peak counting time to background counting time was 2:1. The diameter of the incident beam collimator was 0.5 mm and the crystal to detector distance was 40 cm. The crystallographic data and additional details of data collection and structure determination are summarized in Table 1.

The intensities of three representative reflections which were measured after every 150 reflections remained constant throughout data collection indicating

Table 1

Summary of crystallographic data and intensity collection for **2**, **3**, and **5**

Compound	**2**	**3**	**5**
Empirical formula	$Fe_2C_{38}P_2O_4H_{28}$	$Fe_3C_{42}P_2O_8H_{28}$	$Fe_4C_{44}P_2O_{10}H_{28}$
F_w	722.28	890.17	1002.04
Crystal system	Orthorhombic	Monoclinic	Monoclinic
Space group	$Pbca$ (#61)	$C2/c$ (#15)	$P2_1/n$ (#14)
Z	8	4	4
Cell parameters			
a (Å)	26.27(1)	17.223(7)	11.231(1)
b (Å)	23.18(1)	14.97(2)	21.043(4)
c (Å)	10.938(8)	18.558(3)	20.373(9)
β (deg)	-	108.39(3)	97.373(9)
V (Å^3)	6661(7)	4541(6)	4693(4)
$D_{calc.}$ (g/cm^3)	1.444	1.305	1.347
μ (cm^{-1} with Mo-K_α)	10.03	10.59	13.23
Transmission factor	0.73–1.00	0.95–1.00	0.90–1.00
Scan type	ω–2θ	ω–2θ	ω–2θ
Scan width (ω) (deg)	$0.80 + 0.3 \tan\theta$	$1.31 + 0.3 \tan\theta$	$1.26 + 0.3 \tan\theta$
$2\theta_{max}$ (deg)	55.1	55.2	55.1
No. of reflections measured	8472	5627	11668
No. of reflections observed ($I > 3\sigma(I)$)	3017	3201	6082
$F(000)$	2976	1816	1936
No. of variables	415	249	565
Discrepancy indices			
R [a]	0.057	0.070	0.054
R_w [b]	0.056	0.139	0.071
Goodness of fit indicator [c]	1.74	5.82	3.09
Maximum shift in final cycles	0.07	0.02	0.05

[a] $R = \Sigma\|\|F_o| - |F_c\|| / \Sigma|F_o|$. [b] $R_w = [(\Sigma w(|F_o| - |F_c|)^2 / \Sigma w(F_o^2)]^{1/2}$, where $w = 4F_o^2/\Sigma^2(F_o^2)$. [c] Standard deviation of an observation of unit weight: $[\Sigma w(|F_o| - |F_c|)^2/(N_o - N_v)]^{1/2}$, where N_o = number of observations and N_v = number of variables.

crystal and electronic stability for two crystals. Decay correction was made for compound **5**. Azimuthal scans of several reflections were made and absorption corrections were applied for all three crystals. The data were corrected for Lorentz and polarization effects, including that due to incident beam monochromatization. Of the reflections collected, those with $I > 3\sigma(I)$ were used for structure determination.

The structure was solved by direct methods [17*] and refined by using full-matrix least-squares methods [18*]. The non-hydrogen atoms were refined anisotropically. Hydrogen atoms were included in the structure factor calculation in idealized positions ($d_{C-H}(sp^2) = 0.95$ Å) and were assigned with isotropic thermal parameters which are 20% greater than the B_{eq} value of the atom to which they were bonded. Neutral atoms scattering factors were taken from Cromer and Waber [19].

* Reference number with asterisk indicates a note in the list of references.

Table 2

NMR data for **1–5** [a]

Compound	^{1}H NMR		^{31}P NMR	^{13}C NMR (CO)
	Cp	Phenyl		
1 [b]	4.20 (s, 4H), 4.46 (s, 4H)	7.40–7.64 (m, 20H)	64.8 (s)	220.7 (t, J(P–C) = 9.3 Hz)
2 [b]	4.46 (s, 2H), 4.38 (s, 2H), 3.88 (s, 2H), 3.68 (s, 2H)	7.22–7.49 (m, 20H)	68.4 (s), −15.6 (s)	213.2 (d, J(P–C) = 19 Hz)
3 [b]	4.23 (b, 4H), 3.93 (b, 4H)	7.41–7.44 (m, 20H)	61.6 (s)	213.0 (d, J(P–C) = 19 Hz)
4	4.21 (b, 4H), 3.83 (b, 4H)	7.50–7.26 (m, 20H)	73.5 (s), 64.6 (s)	213.1 (d, J(P–C) = 21 Hz) 213.6 (b)
5	4.47 (b, 4H) 4.06 (b, 4H)	7.67–7.25 (m, 20H)	39.0 (s)	230.8 (m), 216.3 (s)

[a] In $CDCl_3$. Chemical shifts are in ppm. Key: s, singlet; b, broad singlet; m, multiplet; t, triplet; d, doublet. [b] Values taken from ref. 11.

Anomalous dispersion effects were included in $F_{calc.}$ [20]; the values for $\Delta f'$ and $\Delta f''$ were those of Cromer [21]. All calculations were performed using the TEXSAN [22] crystallographic software package at Boston College. The final cycles of refinement led to the R indices listed in Table 1. The final positional and thermal parameters of the non-hydrogen atoms are listed in Table 3, selected interatomic distances and angles are given in Table 4, and complete lists of bond lengths, bond angles, and observed and calculated structure factors are available from the authors.

Results and discussion

Syntheses and characterization

Scheme 1 shows various reaction conditions that lead to the preparation of a new series of iron carbonyls **1–5** demonstrating all possible coordination modes for the ligand BPPF with iron carbonyls.

As the yields and product distribution depended significantly on the reaction conditions, and as the chromatographic separation of these compounds was rather tedious, we have employed a number of experimental procedures to guarantee the preferential formation of any particular compound(s) over others in high yields. Some experimental details of the optimum reaction conditions for the highest yields of **1–3** can be found in our previous report [11]. As illustrated in Scheme 1, a representative procedure is to treat BPPF with $Fe(CO)_5$ in refluxing toluene or benzene for a certain period of time. It was found that the reaction time and temperature played an important role in the product distribution of **1–3**. The longer the reaction time or the higher the reaction temperature, the higher the yields of **2** and **3** achieved at the cost of **1**, suggesting **1** to be thermodynamically less favored than **2** and **3**. In line with these observations is the finding that **1** decomposes readily in solution in air while **2** and **3** remain quite stable for an extended period of time.

When $Fe_2(CO)_9$ and $Fe_3(CO)_{12}$ were treated with BPPF, two new bi- and trinuclear complexes **4** and **5** were formed in addition to the expected products **2** and **3**, although their yields were quite low (< 10%). Interestingly the chelate diphosphine complex **1** was not formed in any observable amount. Thus the results shown in Scheme 1 reveal that chelation is not a choice of preference as far as the reactions of BPPF with iron carbonyls are concerned although there are numerous examples for a chelating diphosphine type complex with this ligand [3,4,6,7,12].

Since the full characterization of **1**–**3**, including X-ray crystallographic analysis of **1**, has already been made in our previous paper, some of their selected NMR data along with those of **4** and **5** are listed in Table 2 for comparative purposes.

The formulation of the heptacarbonyl derivative (**4**) is suggested as such based on microanalytical and NMR data for the compound. The presence of two phosphorus singlets at low field indicates a non-symmetric chelation of BPPF on a single iron atom rather than a symmetric bridging mode, although an AB pattern instead of a pair of singlets would be expected. The room temperature ^{13}C NMR spectrum in the carbonyl region exhibits a broad doublet at 213.1 ppm and a broad singlet at 213.6 ppm. On cooling to −80°C, both signals collapsed into one to give rise to a new multiplet centered at 212.5 ppm, apparently showing a fluxional behavior. The pattern and the numbers of infrared carbonyl stretching bands alone do not show the presence of any bridging carbonyls involved in this dynamic process. Attempts to obtain **4** as crystals suitable for crystallographic studies have so far been frustrating, and the correct solution structure could not be deduced with any certainty.

The decacarbonyl derivative (**5**) exhibits three terminal carbonyl bands at 2067, 1998, and 1952 cm^{-1} and two bridging carbonyl bands at 1782 and 1740 cm^{-1}, the pattern of which is unaltered as compared with that of unsubstituted $Fe_3(CO)_{12}$. The room temperature ^{13}C NMR shows a broad singlet at 216.3 ppm for the four terminal carbonyls located at the unique Fe atom (Fe4 in Fig. 3) and a complex multiplet centered at 230.8 ppm arising from the four terminal and two bridging carbonyls. This reveals the presence of two independent scrambling processes occurring within each group of non-equivalent carbonyls. Lowering the temperature down to −70°C did not significantly alter the pattern of the spectrum except a little further broadening of each signal because of slowing down of the exchange process. An attempt to carry out more extensive variable temperature NMR studies was unsuccessful due to the fact that at the temperatures below −70°C crystals began to deposit from the solution.

Finally, in connection with the ^1H NMR pattern for the cyclopentadienyl ring protons in **1**–**5**, they all exhibit a simple AA′BB′ (or AA′XX′) pattern with the coupling constants $^4J(HH)$ and $^3J(PH)$ negligibly small. Thus a two line pattern in **1**, **3**, **4**, and **5**, and a four line pattern in **2** are exhibited for the AB (or AX) portion.

X-Ray crystal structures of 2, 3, and 5

Apart from the important chemistry of compounds as catalysts [11], the structures of these complexes contain interesting series from the structural viewpoint such as various coordination modes and the environment of the ligand BPPF and Fe atoms, respectively. All crystals contained unsolvated molecules of the complexes except for **3** in which a highly disordered solvent moiety was recognized but

Table 3

Final positional parameters and B_{eq} temperature factors [a] for (η^1-BPPF)Fe(CO)$_4$ (**2**), (μ,η^2-BPPF)(Fe(CO)$_4$)$_2$ (**3**), and (μ,η^2-BPPF)Fe$_3$(CO)$_{10}$ (**5**)

Atom	*x*	*y*	*z*	B_{eq} (Å^2) [b]	Atom	*x*	*y*	*z*	B_{eq} (Å^2) [b]
(a) (η^1-BPPF)Fe(CO)$_4$ (2)									
Fe1	0.6294(1)	0.0143(1)	0.2163(1)	3.06(5)	C20	0.6089(5)	−0.2318(5)	0.2089(14)	9 (1)
Fe2	0.6183(1)	0.2012(1)	0.3991(1)	5.19(7)	C21	0.6281(4)	−0.2147(4)	0.0975(12)	7.3(7)
P1	0.5485(1)	−0.0640(1)	0.0371(1)	3.6(1)	C22	0.6108(3)	−0.1654(4)	0.0440(9)	4.9(5)
P2	0.6699(1)	0.1243(1)	0.4106(2)	3.2(1)	C23	0.7279(3)	0.1255(4)	0.3157(7)	3.3(4)
C1	0.6034(3)	−0.0178(4)	0.0544(6)	3.1(4)	C24	0.7663(3)	0.0868(4)	0.3388(8)	4.3(5)
C2	0.6562(3)	−0.0324(4)	0.0734(6)	3.6(4)	C25	0.8088(3)	0.0863(4)	0.2631(9)	5.5(6)
C3	0.6844(3)	0.0195(4)	0.0869(7)	4.2(4)	C26	0.8128(4)	0.1238(5)	0.1692(9)	6.4(6)
C4	0.6505(3)	0.0663(4)	0.0752(7)	4.1(4)	C27	0.7743(4)	0.1621(5)	0.1474(9)	6.0(6)
C5	0.6014(3)	0.0436(4)	0.0540(7)	3.7(4)	C28	0.7323(3)	0.1640(4)	0.2203(8)	4.1(4)
C6	0.6404(3)	0.0558(4)	0.3791(6)	3.2(4)	C29	0.6954(3)	0.1147(3)	0.5666(7)	3.6(4)
C7	0.5870(3)	0.0473(4)	0.3561(6)	3.3(4)	C30	0.6714(4)	0.0784(4)	0.6463(7)	5.0(5)
C8	0.5783(3)	−0.0122(4)	0.3446(7)	4.1(4)	C31	0.6882(4)	0.0748(4)	0.7665(8)	5.8(6)
C9	0.6248(4)	−0.0409(4)	0.3606(7)	4.1(4)	C32	0.7280(4)	0.1075(5)	0.8041(8)	4.9(5)
C10	0.6633(3)	0.0007(4)	0.3801(7)	4.0(4)	C33	0.7527(3)	0.1431(4)	0.7221(8)	5.1(5)
C11	0.5493(3)	−0.0759(4)	−0.1298(7)	3.3(4)	C34	0.7364(3)	0.1465(4)	0.6057(8)	4.4(5)
C12	0.5360(3)	−0.1298(4)	−0.1764(8)	4.5(5)	C210	0.5813(4)	0.1722(5)	0.5195(10)	6.8(7)
C13	0.5335(3)	−0.1380(4)	−0.3039(9)	5.1(5)	C220	0.6719(5)	0.2449(5)	0.4329(10)	6.8(7)
C14	0.5438(3)	−0.0922(5)	−0.3807(8)	4.9(5)	C230	0.5806(6)	0.2637(6)	0.3932(11)	13 (1)
C15	0.5562(3)	−0.0412(5)	−0.3342(8)	4.8(5)	C240	0.6006(3)	0.1851(4)	0.2451(8)	4.7(5)
C16	0.5589(3)	−0.0322(4)	−0.2082(8)	3.8(4)	O210	0.5564(3)	0.1538(5)	0.5963(8)	11.8(7)
C17	0.5728(3)	−0.1312(4)	0.0984(8)	4.2(5)	O220	0.7063(4)	0.2724(3)	0.4548(8)	10.9(6)
C18	0.5533(4)	−0.1504(4)	0.2053(9)	5.3(6)	O230	0.5590(5)	0.3064(5)	0.3876(9)	17 (1)
C19	0.5713(5)	−0.2000(6)	0.2600(11)	7.4(8)	O240	0.5871(3)	0.1788(3)	0.1488(6)	6.0(4)
(b) (μ,η^2-BPPF)(Fe(CO)$_4$)$_2$ (3)									
Fe1	1.0000	0.4882(2)	0.2500	3.3(1)	C17	0.7120(7)	0.4461(8)	0.1716(7)	3.2(5)
Fe2	0.7524(1)	0.6559(1)	0.1244(1)	3.60(8)	C18	0.7088(8)	0.4369(9)	0.2445(8)	4.2(6)
P1	0.7907(2)	0.5128(2)	0.1517(2)	2.9(1)	C19	0.6482(1)	0.3936(12)	0.2612(10)	6.0(8)
C1	0.8773(7)	0.4942(9)	0.2362(6)	3.3(5)	C20	0.5869(11)	0.3558(11)	0.2028(13)	7 (1)
C2	0.9096(8)	0.4116(9)	0.2700(7)	3.8(6)	C21	0.5861(9)	0.3633(11)	0.1285(11)	6.2(8)
C3	0.9725(8)	0.4286(11)	0.3389(8)	4.5(7)	C22	0.6519(8)	0.4097(10)	0.1133(8)	4.7(7)
C4	0.9800(7)	0.5218(12)	0.3491(7)	4.9(7)	C210	0.6766(10)	0.6154(10)	0.0405(9)	5.7(7)
C5	0.9225(7)	0.5657(9)	0.2862(7)	3.7(6)	C220	0.7398(9)	0.6661(10)	0.2162(9)	4.8(7)
C11	0.8124(7)	0.4478(8)	0.0779(7)	3.1(5)	C230	0.7109(10)	0.7661(10)	0.1025(8)	5.1(7)
C12	0.8179(8)	0.3568(9)	0.0815(8)	4.3(6)	C240	0.8488(10)	0.6921(9)	0.1186(8)	4.7(7)
C13	0.8387(9)	0.3094(10)	0.0256(10)	5.4(7)	O210	0.6299(8)	0.5938(9)	−0.0149(7)	9.6(7)
C14	0.8540(10)	0.3526(12)	−0.0340(10)	5.9(8)	O220	0.7323(7)	0.6771(8)	0.2747(6)	7.5(7)
C15	0.8478(9)	0.4449(12)	−0.0381(8)	5.4(8)	O230	0.6818(9)	0.8339(7)	0.0900(7)	7.8(7)
C16	0.8269(8)	0.4924(9)	0.0173(7)	4.1(6)	O240	0.9111(7)	0.7163(8)	0.1161(7)	6.9(6)
(c) (μ,η^2-BPPF)Fe$_3$(CO)$_{10}$ (5)									
Fe1	0.2544(1)	0.0693(1)	0.1453(1)	2.90(5)	C25	0.7648(8)	0.1105(5)	0.0456(5)	4.9(5)
Fe2	0.2656(1)	0.2922(1)	0.1501(1)	2.97(5)	C26	0.7975(9)	0.1357(5)	−0.0114(6)	4.9(6)
Fe3	0.3718(1)	0.2585(1)	0.0505(1)	2.93(5)	C27	0.7133(9)	0.1644(5)	−0.0566(5)	4.4(5)
Fe4	0.3517(1)	0.3855(1)	0.0747(1)	3.86(6)	C28	0.5959(8)	0.1687(5)	−0.0444(5)	4.0(5)
P1	0.1778(2)	0.2164(1)	0.2082(1)	2.8(1)	C29	0.3206(7)	0.1183(4)	−0.0425(4)	2.9(4)
P2	0.4052(2)	0.1539(1)	0.0320(1)	2.6(1)	C30	0.3706(8)	0.0697(4)	−0.0758(4)	3.5(4)
C1	0.1445(7)	0.1373(4)	0.1764(4)	3.0(4)	C31	0.3040(9)	0.0428(4)	−0.1323(5)	4.1(5)
C2	0.1420(8)	0.0802(5)	0.2161(5)	3.8(4)	C32	0.1881(10)	0.0642(5)	−0.1557(5)	4.7(5)
C3	0.1044(8)	0.0293(5)	0.1745(6)	4.4(5)	C33	0.1409(9)	0.1123(6)	−0.1206(6)	5.3(6)
C4	0.0799(8)	0.0524(5)	0.1079(5)	4.5(5)	C34	0.2052(8)	0.1393(5)	−0.0657(5)	4.1(5)

Table 3 (continued)

Atom	x	y	z	B_{eq} (Å^2) [b]	Atom	x	y	z	B_{eq} (Å^2) [b]
C5	0.1054(7)	0.1189(4)	0.1081(5)	3.4(4)	C200	0.4209(8)	0.2560(4)	0.1527(4)	3.2(4)
C6	0.3937(7)	0.0926(4)	0.0942(4)	2.8(4)	C210	0.1304(10)	0.3375(5)	0.1341(5)	4.7(5)
C7	0.4272(7)	0.0981(4)	0.1652(4)	3.4(4)	C220	0.3145(9)	0.3350(5)	0.2240(5)	4.3(5)
C8	0.4115(8)	0.0372(5)	0.1935(5)	4.0(5)	C300	0.2027(8)	0.2564(4)	0.0569(5)	3.6(4)
C9	0.3692(8)	−0.0055(4)	0.1428(5)	4.1(5)	C310	0.3380(9)	0.2729(4)	−0.0363(5)	4.4(5)
C10	0.3573(8)	0.0276(4)	0.0810(4)	3.4(4)	C320	0.5265(9)	0.2787(4)	0.0525(5)	3.9(4)
C11	0.2471(7)	0.2012(4)	0.2943(4)	3.0(4)	C410	0.4392(10)	0.4148(5)	0.0127(6)	4.8(6)
C12	0.1788(8)	0.1788(5)	0.3417(5)	4.0(5)	C420	0.2172(10)	0.3801(5)	0.0148(5)	4.7(5)
C13	0.2328(11)	0.1664(5)	0.4065(5)	5.2(6)	C430	0.3015(11)	0.4564(5)	0.1109(6)	5.6(6)
C14	0.3546(11)	0.1777(6)	0.4246(6)	6.2(7)	C440	0.4780(10)	0.3833(5)	0.1398(5)	4.9(5)
C15	0.4210(9)	0.1999(6)	0.3774(6)	5.6(6)	O200	0.5101(5)	0.2422(3)	0.1867(3)	3.8(3)
C16	0.3686(8)	0.2112(5)	0.3135(5)	4.3(5)	O210	0.0435(7)	0.3666(4)	0.1251(4)	8.1(5)
C17	0.0288(7)	0.2450(4)	0.2210(4)	3.2(4)	O220	0.3425(7)	0.3646(4)	0.2725(4)	6.5(4)
C18	−0.0727(8)	0.2232(5)	0.1835(5)	5.0(5)	O300	0.1062(5)	0.2476(3)	0.0275(3)	4.1(3)
C19	−0.1838(9)	0.2479(7)	0.1911(7)	7.4(7)	O310	0.3189(8)	0.2833(4)	−0.0933(4)	7.4(5)
C20	−0.1938(10)	0.2935(7)	0.2389(6)	6.8(7)	O320	0.6252(6)	0.2925(3)	0.0526(3)	5.4(4)
C21	−0.0932(10)	0.3162(6)	0.2768(5)	6.0(6)	O410	0.4959(8)	0.4321(4)	−0.0272(4)	7.2(5)
C22	0.0177(9)	0.2926(5)	0.2678(5)	4.8(5)	O420	0.1329(7)	0.3826(4)	−0.0238(4)	6.3(4)
C23	0.5599(7)	0.1419(4)	0.0138(4)	3.0(4)	O430	0.2682(9)	0.5008(4)	0.1336(5)	9.5(6)
C24	0.6443(8)	0.1135(4)	0.0582(5)	3.7(4)	O440	0.5585(7)	0.3873(4)	0.1799(4)	6.5(4)

[a] Numbers in parentheses are the estimated standard deviations in the units of the least significant figure given for the corresponding parameter. [b] B_{eq}'s for anisotropically refined atoms are given in the form of the isotropic equivalent displacement parameter defined as $(4/3)[a^2\beta_{11} + b^2\beta_{22} + c^2\beta_{33} + (2ab\cos\gamma)\beta_{12} + (2ac\cos\beta)\beta_{13} + (2bc\cos\alpha)\beta_{23}]$.

not identified in any forms. However, the positions of the atoms in ligand BPPF and iron carbonyls are highly refined as shown in their esd's of positional parameters and selected structural data.

As found in other metal carbonyl complexes of BPPF [13,14], the ligand BPPF provides several types of coordination modes in which BPPF should possess two kinds of freedoms for adjusting the coordination mode to minimize the strains of BPPF caused by the complexation to the Fe atom, that is, the rotation around the Cp–Fe–Cp axis (Scheme 2) and the tilt of the two Cp rings. With these structural freedoms, BPPF can adjust its bite angle and/or distance between two metal atoms which BPPF bridges. With the previously reported bidentate structure of BPPF in **1**, the iron carbonyl complexes **2**, **3**, and **5** provide new coordination modes of BPPF as monodentate (**2**) and bridging modes (**3** and **5**), as shown in Figs. 1–3, respectively. The selected principal bond lengths and angles are tabulated in Table 4.

The Fe atom of iron carbonyl in each structure is at the center of the trigonal bipyramid environment. The distortion from ideal geometry is dependent on the coordination modes of BPPF. As suggested with a bidentate BPPF with one iron carbonyl, the most severe distortion from the ideal trigonal bipyramidal geometry is found in **1** (168.2(3)°, angle between two atoms in axial positions (P1–Fe2–C1)). A small distortion is found in **3** with bridging mode of BPPF (173.8(5)°) and in **2** with monodentate BPPF (176.9(5)°). The coordination environment of Fe atoms in

Table 4

Selected bond lengths (Å) and bond angles (°) [a] for **2**, **3**, and **5**

Bonds and angles	**2**	**3**	**5**
Selected bond lengths (Å)			
Fe1–C1	2.040(7)	2.05(1)	2.039(8)
Fe1–C2	2.029(7)	2.06(1)	2.028(8)
Fe1–C3	2.025(8)	2.06(1)	2.034(9)
Fe1–C4	2.034(8)	2.04(1)	2.04(1)
Fe1–C5	2.038(8)	2.04(1)	2.031(9)
Fe1–C6	2.042(7)	–	2.036(8)
Fe1–C7	2.040(7)	–	2.023(9)
Fe1–C8	2.037(8)	–	2.015(9)
Fe1–C9	2.037(8)	–	2.039(8)
Fe1–C10	2.025(8)	–	2.036(8)
Fe2–C200	–	–	1.897(9)
Fe2–C210	1.77(1)	1.79(2)	1.79(1)
Fe2–C220	1.77(1)	1.79(2)	1.76(1)
Fe2–C230	1.75(1)	1.79(2)	–
Fe2–C240	1.79(1)	1.78(2)	–
Fe2–C300	–	–	2.05(1)
Fe3–C200	–	–	2.052(9)
Fe3–C300	–	–	1.920(9)
Fe3–C310	–	–	1.76(1)
Fe3–C320	–	–	1.78(1)
Fe4–C410	–	–	1.79(1)
Fe4–C420	–	–	1.81(1)
Fe4–C430	–	–	1.78(1)
Fe4–C440	–	–	1.80(1)
Fe2–Fe3	–	–	2.553(2)
Fe2–Fe4	–	–	2.728(2)
Fe3–Fe4	–	–	2.730(2)
Fe2–P1	–	2.251(5)	2.266(3)
Fe2–P2	2.243(3)	–	–
Fe3–P2	–	–	2.270(3)
P1–C1	1.807(8)	1.81(1)	1.813(9)
P1–C11	1.846(8)	1.81(1)	1.828(8)
P1–C17	1.811(9)	1.81(1)	1.825(8)
P2–C6	1.801(8)	–	1.809(8)
P2–C23	1.844(8)	–	1.836(8)
P2–C29	1.847(8)	–	1.824(8)
C200–O200	–	–	1.17(1)
C210–O210	1.15(1)	1.14(2)	1.15(1)
C220–O220	1.13(1)	1.14(2)	1.16(1)
C230–O230	1.14(1)	1.12(2)	–
C240–O240	1.12(1)	1.15(2)	–
C300–O300	–	–	1.18(1)
C310–O310	–	–	1.16(1)
C320–O320	–	–	1.15(1)
C410–O410	–	–	1.14(1)
C420–O420	–	–	1.14(1)
C430–O430	–	–	1.12(1)
C440–O440	–	–	1.13(1)

Table 4 (continued)

Bonds and angles	2	3	5
Selected bond angles (deg)			
P2–Fe2–C210	89.3(4)	–	–
P2–Fe2–C220	87.9(4)	–	–
P2–Fe2–C230	176.9(5)	–	–
P2–Fe2–C240	92.5(3)	–	–
P1–Fe2–C200	–	–	99.8(3)
P1–Fe2–C210	–	87.4(5)	92.8(3)
P1–Fe2–C220	–	89.0(5)	92.1(3)
P1–Fe2–C230	–	89.2(7)	–
P1–Fe2–C240	–	95.2(5)	–
P1–Fe2–C300	–	–	95.0(3)
C200–Fe2–C210	–	–	167.4(4)
C200–Fe2–C220	–	–	89.8(4)
C200–Fe2–C300	–	–	93.9(4)
C200–Fe2–P1	–	–	99.5(3)
C200–Fe2–Fe3	–	–	52.3(3)
C200–Fe2–Fe4	–	–	85.1(3)
C210–Fe2–C220	119.9(5)	125.7(7)	92.5(5)
C210–Fe2–C230	91.8(6)	89.2(7)	–
C210–Fe2–C240	118.6(5)	119.1(7)	–
C220–Fe2–C230	89.1(7)	88.7(6)	–
C220–Fe2–C240	121.5(5)	115.2(7)	–
C230–Fe2–C240	89.5(5)	91.3(7)	–
C300–Fe2–C210	–	–	81.2(4)
C300–Fe2–C220	–	–	170.7(4)
C300–Fe2–P1	–	–	95.0(3)
C300–Fe2–Fe3	–	–	47.8(2)
C300–Fe2–Fe4	–	–	82.3(3)
P1–Fe2–Fe3	–	–	118.97(8)
P1–Fe2–Fe4	–	–	174.96(9)
Fe3–Fe2–Fe4	–	–	62.16(5)
P2–Fe3–Fe2	–	–	120.02(8)
P2–Fe3–Fe4	–	–	175.28(8)
Fe2–Fe3–Fe4	–	–	62.07(5)
C200–Fe3–Fe2	–	–	47.1(2)
C200–Fe3–Fe4	–	–	82.2(3)
C200–Fe3–P2	–	–	96.3(3)
C300–Fe3–Fe2	–	–	52.3(3)
C300–Fe3–Fe4	–	–	84.6(3)
C300–Fe3–P2	–	–	100.0(3)
Fe2–Fe4–Fe3	–	–	55.77(4)
C1–P1–Fe2	–	116.3(4)	123.3(3)
C1–P1–C11	100.5(3)	105.2(5)	102.1(4)
C1–P1–C17	101.0(4)	101.7(5)	101.4(4)
C11–P1–Fe2	–	117.2(4)	116.7(3)
C11–P1–C17	103.6(4)	101.8(6)	102.3(4)
C17–P1–Fe2	–	112.6(4)	108.2(3)
C6–P2–Fe2	115.5(3)	–	–
C6–P2–C23	105.1(3)	–	101.5(4)
C6–P2–C29	103.1(4)	–	101.2(4)
C23–P2–Fe2	117.1(3)	–	–
C23–P2–C29	102.8(4)	–	101.1(4)
C29–P2–Fe2	111.5(3)	–	–

Table 4 (continued)

Bonds and angles	2	3	5
C6–P2–Fe3	–	–	123.4(3)
C23–P2–Fe3	–	–	109.6(3)
C29–P2–Fe3	–	–	116.9(3)
O200–C200–Fe2	–	–	145.9(7)
O200–C200–Fe3	–	–	133.3(7)
Fe2–C200–Fe3	–	–	80.4(3)
O210–C210–Fe2	178(1)	176(2)	179(1)
O220–C220–Fe2	180(1)	177(1)	177(1)
O230–C230–Fe2	175(2)	177(2)	–
O240–C240–Fe2	174.4(8)	179(1)	–
O300–C300–Fe2	–	–	134.3(7)
O300–C300–Fe3	–	–	145.4(8)
Fe2–C300–Fe3	–	–	79.9(4)

[a] The numbers in parentheses are the estimated standard deviations in the units of the least significant digit given for the corresponding parameters.

5 is very complicated and is similar to those found in $Fe_3(CO)_{12}$ (see below) [23,24]. All carbon atoms of carbonyls in the three crystal structures are about 1.78(1) Å (average) apart from the central iron atom, with no particular differences in their equatorial and axial positions. Only their angles with adjacent ligands distinguish their position.

The bond distances between Fe and P atoms are 2.243(3), 2.251(5), and 2.266(3) and 2.270(3) Å for complexes **2**, **3** and **5**, respectively, showing quite similar distances to those found in complex **1** (2.243(3) and 2.256(3) Å) [11] and (dppe)$Fe(CO)_3$ [25] and small elongation of those found in **5**, as expected in the coordination of BPPF with the bulkier $Fe_3(CO)_{10}$ moiety.

The ferrocene portion of BPPF ligands in the crystal structures of the four molecules showed various kinds of geometries with the rotation around axes perpendicular to the centers of the two cyclopentadienyl rings and Fe atoms, demonstrating its structural flexibility which is dependent on the coordination modes of BPPF ligand to Fe atoms of additional iron carbonyls. In complex **1** (bidentated BPPF) and **5** (bridged to the same $Fe_3(CO)_{10}$ moiety), the rotation is somewhat limited showing +7.5 and +61.6° of rotation from Type I in Scheme 2 with preference for the eclipsed form (+7.5 and −10.4° from a complete eclipsed form of Types I and III in Scheme 2, respectively). When they are, however, either monodentated (**2**) or bridged to two separated iron carbonyls through P atoms (**3**), their rotational freedoms are greatly increased to give almost opposite ligational direction (+132.79 and 162.85° rotation from Type I and −11.21 and +18.85 rotation from Type V, respectively for the complexes **2** and **3**). All ferrocenes in three (**1**, **2**, and **5**) out of these four complexes have preferential geometry of eclipsed forms (see above), while that in **3** has a geometry almost in the middle of the eclipsed and staggered forms (+18.85 and −17.15° rotation from Types V and VI, respectively).

In all compounds, the cyclopentadienyl rings are planar within experimental error but show slight deviations from being parallel to each other; 2.2, 2.64, 1.65, 3.07° for compounds **1**, **2**, **3**, and **5**, respectively. This non-coplanarity is probably

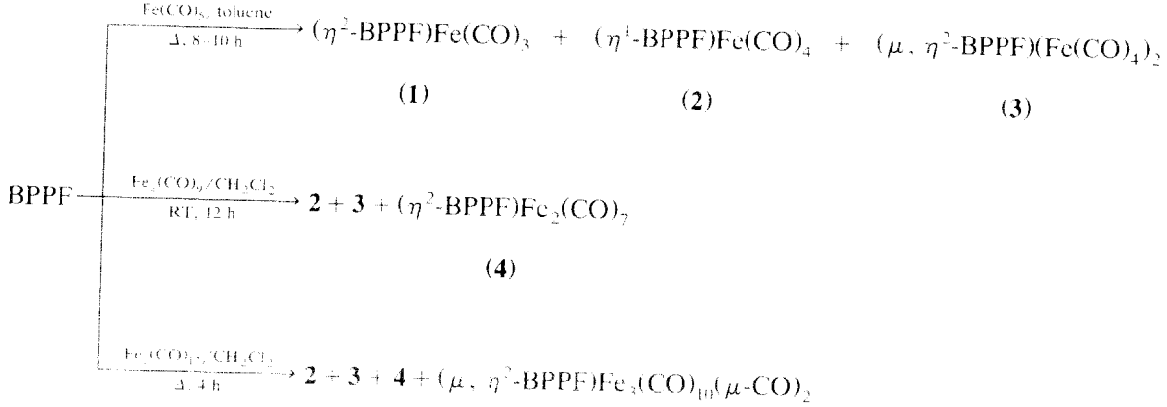
BPPF
Fe(CO)5, toluene
Δ, 8–10 h
(η2-BPPF)Fe(CO)3 + (η1-BPPF)Fe(CO)4 + (μ, η2-BPPF)(Fe(CO)4)2
(1)
(2)
(3)
Fe2(CO)9/CH2Cl2
RT, 12 h
2 + 3 + (η2-BPPF)Fe2(CO)7
(4)
Fe3(CO)12/CH2Cl2
Δ, 4 h
2 + 3 + 4 + (μ, η2-BPPF)Fe3(CO)10(μ-CO)2
(5)

Scheme 1

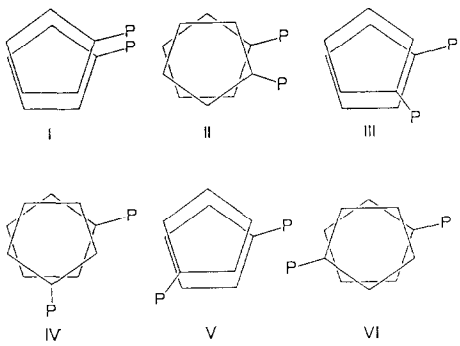

Scheme 2

caused by the displacement of the phosphine substitutes from the cyclopentadienyl rings (+0.12 Å on average).

P–C bond lengths are slightly different depending on the kinds of rings in which the C atoms belong. With C atoms of cyclopentadienyl rings, P–C bond lengths are slightly shorter (1.801–1.810 Å) than those with C of phenyl rings (1.823–1.857 Å). These differences were also recognized in the Pd, Ni, Mo complexes of iron carbonyls [26]. Angles at P atoms are distinguished by two types; 103 and 113° for C–P–C and C–P–Fe, respectively. The C–C bond lengths and C–C–C angles in cyclopentadienyl rings are well in the range of those reported and do not show any particular effect of substitution. Bond lengths and angles in the phenyl rings are within the ranges usually found.

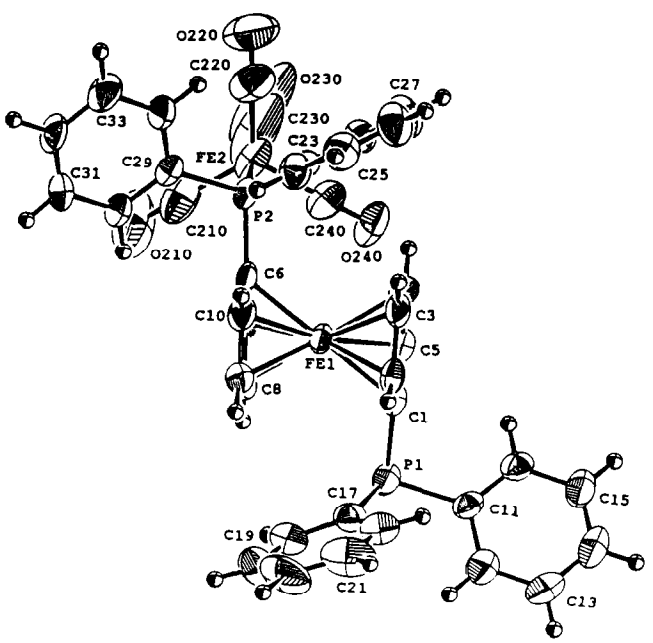

Fig. 1. Molecular structure of $(\eta^1$-BPPF)Fe$(CO)_4$ (**2**). Atoms are represented by 50% probability thermal ellipsoids.

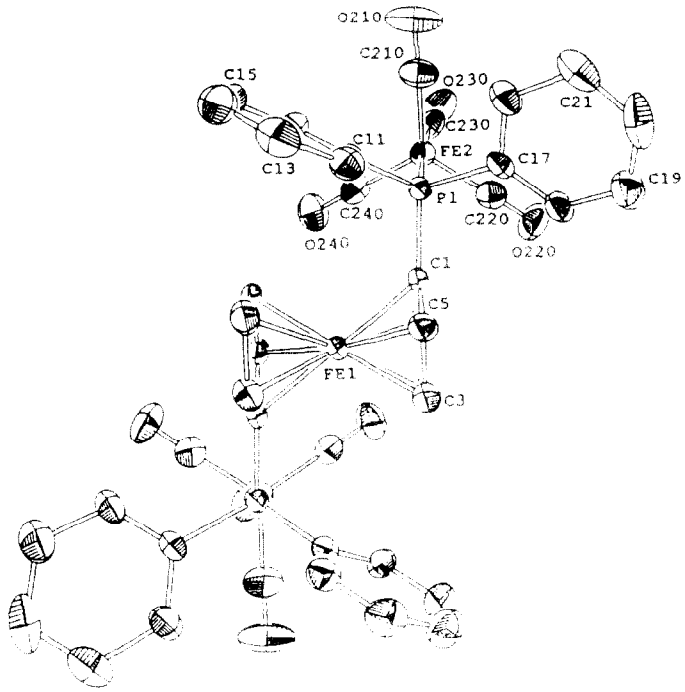

Fig. 2. Molecular structure of $(\mu,\eta^2$-BPPF)Fe$(CO)_4$ (**3**). Atoms are represented by 50% probability thermal ellipsoids.

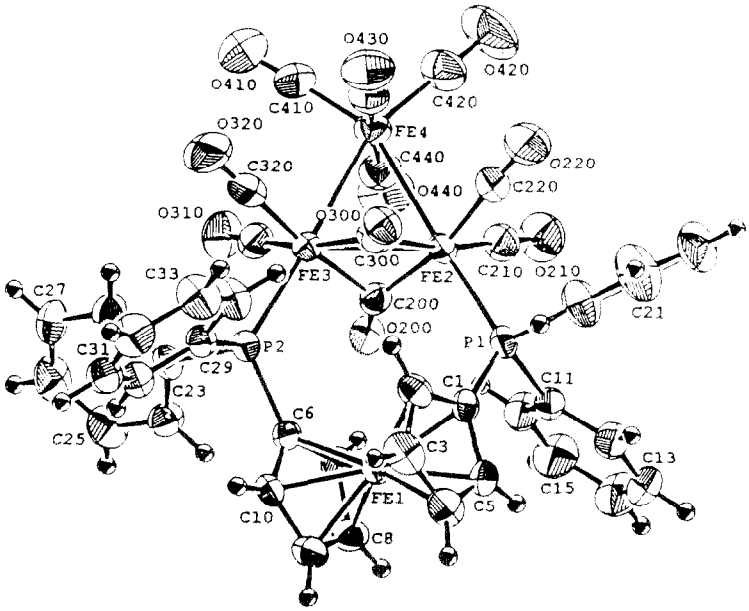

Fig. 3. Molecular structure of $(\mu,\eta^2$-BPPF)$Fe_3(CO)_{10}$ (**5**). Atoms are represented by 50% probability thermal ellipsoids.

The triiron decacarbonyl moiety of complex **5** is found to be ordered, unlike the disorders found in two previous structural studies of $Fe_3(CO)_{12}$ [23,24]. With relatively high resolution ($2\theta_{max}$ as high as 55.1°), the structure of the iron carbonyl moiety shows a triangle of Fe atoms and 8 terminal and 2 bridged carbonyls with a total of approximate C_{2v} symmetry. However, a close examination of the two bridged carbonyls lowered the symmetry to C_2 (see Table 4 for structural data around the two carbonyls). All terminal carbonyls have essentially linear conformation (average Fe–C–O angles of 177°), while the two bridged ones have angles of 145.7 and 133.8°, respectively, toward two Fe atoms in the cluster. Marginal difference in bond lengths of CO between terminal and bridged ones was recognized (1.13 and 1.18 Å, respectively, on average).

Finally, the Fe–Fe distances in complex **5** are 2.553(2) Å for the one with bridging carbonyls and P atoms of BPPF, 2.728(2) and 2.730(2) Å for the ones without such bridging carbonyls in between. Interestingly, the four Fe atoms of the complex are located almost on the same plane; 0.05 Å (Fe of ferrocene) above the least-square plane of the three Fe atoms of $Fe_3(CO)_{10}$ moiety.

Acknowledgments

TJK gratefully acknowledges the Korea Science and Engineering Foundation for financial support (Grant No. 88-0304-03). NHH expresses a sincere gratitude to MMT for travel and financial support.

References

1 M. Kumada, T. Hayashi and K. Tamao, Fundamental Research in Homogeneous Catalysis, Plenum, New York, 1982, p. 175.
2 T. Hayashi and M. Kumada, Acc. Chem. Res., 15 (1982) 395.
3 W.R. Cullen, F.W.B. Einstein, T. Jones and T.J. Kim, Organometallics, 2 (1983) 741.
4 W.R. Cullen, F.W.B. Einstein, T. Jones and T.J. Kim, Organometallics, 4 (1985) 346.
5 T.G. Appleton, W.R. Cullen, S.V. Evans, T.J. Kim and J. Trotter, J. Organomet. Chem., 279 (1985) 5.
6 T.J. Kim and K.C. Lee, Bull. Korean Chem., 10 (1989) 279.
7 T. Hayashi, M. Konishi, Y. Kobori, M. Kumada, T. Higuchi and K. Hirotsu, J. Am. Chem. Soc., 106 (1984) 158.
8 W.R. Cullen, S.V. Evans, N.F. Han and J. Trotter, Inorg. Chem., 26 (1987) 514.
9 Y. Ito, M. Sawamura and T. Hayashi, J. Am. Chem. Soc., 108 (1986) 6405.
10 Y. Ito, M. Sawamura and T. Hayashi, Tetrahedron Lett., 289 (1987) 6215.
11 T.J. Kim, K.H. Kwon, S.C. Kwon, J.O. Baeg, S.C. Shim and D.H. Lee, J. Organomet. Chem., 389 (1990) 205.
12 W.R. Cullen and J.D. Woolins, Coord. Chem. Rev., 39 (1981) 1.
13 D.J. Hill, G.R. Girard, F.L. McCabe, R.K. Johnson, P.D. Stupik, J.H. Zhang, W.M. Reiff and D.S. Eggleston, Inorg. Chem., 28 (1989) 3529.
14 S. Onaka, A. Mizano and S. Takagi, Chem. Lett., 1989, 2037.
15 D.D. Perin, W.L.F. Armarego and D.R. Perin, Purification of Laboratory Chemicals, 2nd ed., Pergamon, New York, 1980.
16 T.J. Bishop, A. Davison, M.L. Katcher, D.W. Lichtenberg, R.E. Merril and J.C. Smart, J. Organomet. Chem., 27 (1971) 241.
17 Programs used are MITRILL, an integrated direct methods computer program (C.J. Gilmore, J. Appl. Crystallogr., 17 (1984) 42) and DIRDIF, an automatic procedure for phase extension and refinement of difference structure factors (P.T. Berntskens, Technical Report 1984/1, Crystallography Laboratory, Toernooiveld, 6525 ED Nijmegen, Netherlands).

18 Function minimized: $\sum w(|F_o| - |F_c|)^2$, where $w = 4F_o^2/\sigma^2(F_o^2)$, $\sigma^2(F_o^2) = [S^2(C + R^2B) + (pF_o^2)^2]/L_p^2$, where S = scan rate, C = total integrated peak count, R = ratio of scan time to background counting time, B = total background count, L_p = Lorentz polarization factor, and p = p-factor.
19 D.T. Cromer and J.T. Waber, International Tables for X-Ray Crystallography, Vol. IV, The Kynoch Press, Birmingham, England, 1974, Table 2.2A.
20 J.A. Ibers and W.C. Hamilton, Acta Crystallogr., 17 (1964) 781.
21 D.T. Cromer, International Tables for X-Ray Crystallography, Vol. IV, The Kynoch Press, Birmingham, England, 1974, Table 2.3.1.
22 TEXSAN–TEXRAY Structural Analysis Package, Molecular Structure Corporation, 1985.
23 C.H. Wei and L.F. Dahl, J. Am. Chem. Soc., 91 (1969) 1351.
24 F.A. Cotton and J.M. Troup, J. Am. Chem. Soc., 94 (1974) 4155.
25 R.P. Battaglia, D. Delledonne, M. Nardelli, C. Pelizzi, G. Predieri and G.P.L. Chiusoli, J. Organomet. Chem., 330 (1987) 101.
26 I.R. Butler, W.R. Cullen, T.J. Kim, S.J. Rettig and J. Trotter, Organometallics, 4 (1985) 972.